Optical-axis perturbation in triaxial ring resonator

Jie Yuan,[1,*] Xingwu Long,[1] and Linmei Liang[2]

[1]Department of Optoelectronic Engineering, College of Optoelectronic Science and Engineering, National University of Defense Technology, Changsha 410073, China
[2]College of Science, National University of Defense Technology, Changsha 410073, China

*Corresponding author: jieyuan@nudt.edu.cn

Received 10 August 2007; revised 26 October 2007; accepted 4 December 2007; posted 7 December 2007 (Doc. ID 85838); published 1 February 2008

We report several findings on the optical-axis perturbation of monolithic triaxial ring resonator. A criterion, C, which represents the mismatching error of the monolithic triaxial ring resonator, has been found out and it cannot be decreased by modifying the angles of the terminal surfaces or the terminal mirrors of the resonator. When $C \neq 0$, an optimization method to share the mismatching error C in some specific directions equally and simultaneously has been proposed. The interesting findings are important to cavity design, cavity improvement, and alignment of the monolithic triaxial ring resonator. © 2008 Optical Society of America

OCIS codes: 140.4780, 140.3410, 140.3370, 140.3560.

1. Introduction

One of the many successful uses of laser is as a rotate sensor. There have been many kinds of planar or nonplaner monoaxial ring resonators, which are widely used for laser gyroscopes [1–4]. Some applications need small size without compromising accuracy too much. The construction of a triaxial ring laser gyro in a single optical block leads to a better compromise between accuracy and small size.

There has been extensive research on the mirror misalignment-induced optical-axis perturbation of planar or nonplanar ring resonators [5–14]. All of the above-referenced articles are concerned only with the monoaxial ring resonator. A monolithic triaxial ring resonator [15] is shown in Fig. 1. Since each mirror of the monolithic triaxial ring resonator is used for two optical cavities, the misalignment of every single mirror will bring the optical-axis perturbation to two related optical cavities. This brings more complexity. The optical-axis perturbation of this monolithic triaxial ring resonator has not been analyzed before.

A mathematic model of a monolithic triaxial ring resonator has been established in this paper. By utilizing the result of a monoaxial ring resonator obtained in our previous papers and following the extended matrix formulation [11,14,16,17], the optical-axis perturbations at several symmetrical points of the monolithic triaxial ring resonator will be analyzed in detail. The interrelationship in the optical-axis perturbations of the three monoaxial ring resonators will also be discussed in detail. A criterion, C, which represents the mismatching error of the monolithic triaxial ring resonator, will be found. When the mismatching error C is not equal to 0, an optimization method to share the mismatching error C will be obtained. The results in this paper are important to cavity design, cavity improvement, and alignment of the monolithic triaxial ring resonator.

2. Analysis Method and Results

As shown in Fig. 1, a monolithic triaxial ring cavity is chosen for analysis [15]. Mirrors M_1, M_2, M_3, M_4, M_5, and M_6 are positioned in the center of each cube body face. The cube is machined such that a small diameter bore connects adjacent mirrors. A closed optical cavity is defined between four coplanar mirrors, which are interconnected by bores. There are three mutually orthogonal closed beam paths, each of which is used to detect angular rotation about its normal axis. The planar ring resonator that is defined by the optical cavity between the mirrors M_2, M_3, M_4, and M_6 is called cavity A; the resonator defined by M_1, M_3, M_5, and M_6 is called cavity B; and the resonator defined by M_1, M_2, M_5, and M_4 is called cavity C. The

0003-6935/08/050628-04$15.00/0

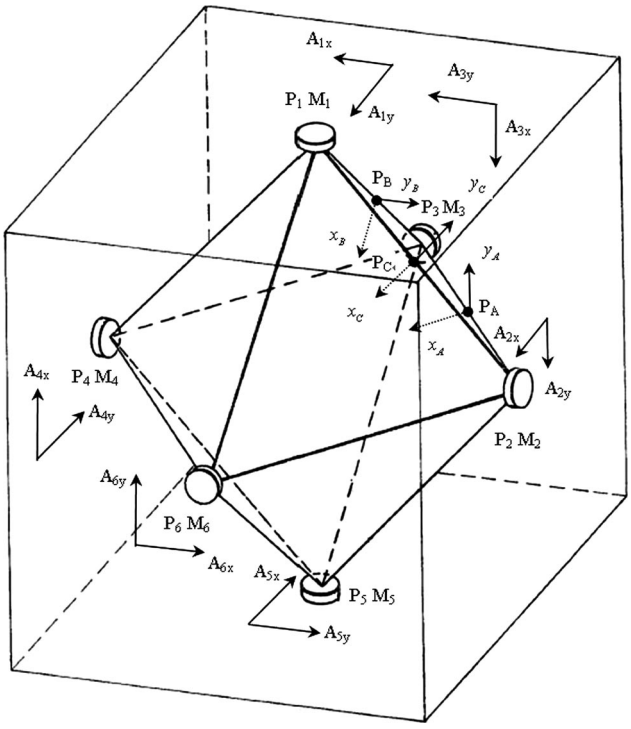

Fig. 1. Schematic of monolithic triaxial ring resonator.

mirrors M_1, M_2, and M_3 are spherical mirrors with common radius R, and the mirrors M_4, M_5, and M_6 are chosen to be flat. Points P_1, P_2, P_3, P_4, P_5, and P_6 are the terminal points of the resonator. The diaphragms of cavities A, B, and C are, respectively, located at points P_A, P_B, and P_C, which are the midpoints between the two spherical mirrors M_2, M_3, or M_1. For a monolithic triaxial ring cavity, it would be better if the optical axes of all three monoaxial ring resonators pass through the center of their diaphragms simultaneously.

All three planar ring resonators are square ring resonators that are mutually orthogonal. A square ring resonator is shown in Fig. 2. The mirrors M_a and M_b are spherical mirrors, and the mirrors M_c and M_d are flat mirrors. The incidence angle is 45°. Points P_a, P_b, P_c, and P_d are the terminal points of the resonator. The diaphragm is located at point P_e, which is the midpoint between the two spherical mirrors P_a and P_b. The optical-axis perturbation at point P_e caused by the spherical and planar mirror's misalignments can be written as [11,14]

$$\Delta x_e = \frac{\sqrt{2}}{4} R(\theta_{ax} + \theta_{bx} + \theta_{cx} + \theta_{dx}), \tag{1}$$

$$\Delta y_e = \frac{\sqrt{2}}{2} R(\theta_{ay} + \theta_{by} + \theta_{cy} + \theta_{dy}). \tag{2}$$

The optical-axis locations x_e and y_e are the optical-axis deviations from the longitudinal axis of the ideal diaphragm along the x and y axes, respectively. Δx_e and Δy_e are the optical-axis perturbations in the axes of x and y, respectively. θ_{ix} and θ_{iy} are the misalignment angles of mirror i ($i = a, b, c, d$) in its local tangential and sagittal planes, respectively. Their positive orientations are defined as follows. As shown in Fig. 2, the positive orientation of y_e is upward and perpendicular to the plane of the resonator. The positive orientation of x_e is shown as the black arrow located at point P_c. The misalignment angles of θ_{ax}, θ_{ay}, θ_{bx}, θ_{by}, θ_{cx}, θ_{cy}, θ_{dx}, and θ_{dy} are defined as follows. We choose point a as an example and a spherical mirror P_a is located at point a. As shown in Figs. 2 and 3(a), to define the misalignment angles of θ_{ax} and θ_{ay}, two orthogonal rotation axes A_{ax} and A_{ay} have been defined for the mirror M_a. The two rotation axes A_{ax} and A_{ay} are in the plane of the mirror M_a. When we look at the mirror in front of the rotation axis A_{ax}, the mirror is shown as Figs. 3(b) and 3(c). When the mirror rotates clockwise with respect to its rotation axis A_{ax}, the induced misalignment angle of θ_{ax} is positive and it is shown in Fig. 3(b), i.e., $\theta_{ax} > 0$. When the mirror rotates counterclockwise with respect to its rotation axis A_{ax}, the induced misalignment angle of θ_{ax} is negative and it is shown in Fig. 3(c), i.e., $\theta_{ax} < 0$. The misalignment angles of θ_{ay}, θ_{bx}, θ_{by}, θ_{cx}, θ_{cy}, θ_{dx}, and θ_{dy} are defined similarly.

Based on the above discussion, we can discuss the optical-axis perturbation of the monolithic triaxial ring resonator. Points P_A, P_B, and P_C, which are the diaphragms of the cavities A, B, and C, are chosen for analysis. As shown in Fig. 1, the positive orientations of x_A, y_A, x_B, y_B, x_C, and y_C are parallel to the directions of the vectors $\overrightarrow{P_2P_6}$, $\overrightarrow{P_5P_1}$, $\overrightarrow{P_1P_6}$, $\overrightarrow{P_4P_2}$, $\overrightarrow{P_2P_5}$, and $\overrightarrow{P_6P_3}$, respectively. The misalignment angles of θ_{ix} and θ_{iy} ($i = 1, 2, 3, 4, 5, 6$) are defined as follows. We choose point P_1 as an example and a spherical mirror M_1 is located at point P_1. The induced misalignment angle of θ_{1x} is positive when the spherical mirror rotates clockwise with respect to its rotation axis A_{1x}. The induced misalignment angle of θ_{1x} is negative when

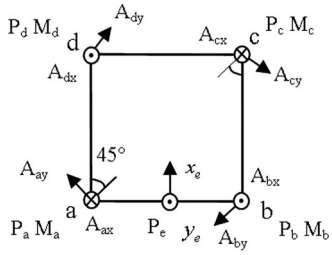

Fig. 2. Schematic of a square ring resonator.

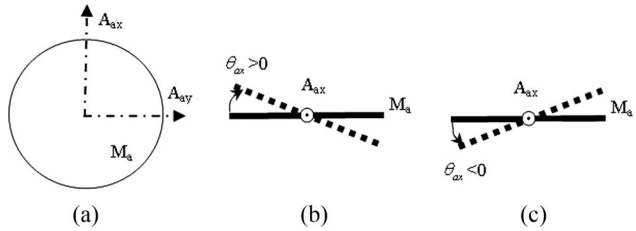

Fig. 3. Definition of the mirror's misalignments angle θ_{ax}.

the spherical mirror rotates counterclockwise with respect to its rotation axis A_{1x}. The misalignment angles of θ_{2x}, θ_{2y}, θ_{3x}, θ_{3y}, θ_{4x}, θ_{4y}, θ_{5x}, θ_{5y}, θ_{6x}, and θ_{6y} are defined similarly. The directions of rotation axes A_{1x}, A_{1y}, A_{2x}, A_{2y}, A_{3x}, A_{3y}, A_{4x}, A_{4y}, A_{5x}, A_{5y}, A_{6x}, and A_{6y} are parallel to the directions of the vectors $\overrightarrow{P_2P_4}$, $\overrightarrow{P_3P_6}$, $\overrightarrow{P_3P_6}$, $\overrightarrow{P_1P_5}$, $\overrightarrow{P_1P_5}$, $\overrightarrow{P_2P_4}$, $\overrightarrow{P_5P_1}$, $\overrightarrow{P_6P_3}$, $\overrightarrow{P_6P_3}$, $\overrightarrow{P_4P_2}$, $\overrightarrow{P_4P_2}$, and $\overrightarrow{P_5P_1}$, respectively. The optical-axis perturbations at points P_A, P_B, and P_C caused by the spherical and planar mirror's misalignments can be written as

$$\Delta x_A = \frac{\sqrt{2}}{4} R(\theta_{2y} - \theta_{3x} - \theta_{4x} + \theta_{6y}),$$

$$\Delta y_A = \frac{\sqrt{2}}{2} R(\theta_{2x} - \theta_{3y} + \theta_{4y} - \theta_{6x}), \tag{3}$$

$$\Delta x_B = \frac{\sqrt{2}}{4} R(\theta_{3y} - \theta_{1x} - \theta_{6x} + \theta_{5y}),$$

$$\Delta y_B = \frac{\sqrt{2}}{2} R(\theta_{3x} - \theta_{1y} + \theta_{6y} - \theta_{5x}), \tag{4}$$

$$\Delta x_C = \frac{\sqrt{2}}{4} R(\theta_{1y} - \theta_{2x} - \theta_{5x} + \theta_{4y}),$$

$$\Delta y_C = \frac{\sqrt{2}}{2} R(\theta_{1x} - \theta_{2y} + \theta_{5y} - \theta_{4x}). \tag{5}$$

If we let

$$x'_A = x_A, \quad y'_A = y_A/2, \quad x'_B = x_B, \quad y'_B = y_B/2,$$
$$x'_C = x_C, \quad y'_C = y_C/2. \tag{6}$$

Then,

$$\Delta x'_A = \Delta x_A, \quad \Delta y'_A = \Delta y_A/2, \quad \Delta x'_B = \Delta x_B,$$
$$\Delta y'_B = \Delta y_B/2, \quad \Delta x'_C = \Delta x_C, \quad \Delta y'_C = \Delta y_C/2, \tag{7}$$

we can obtain

$$\Delta x'_A + \Delta y'_A + \Delta x'_B + \Delta y'_B + \Delta x'_C + \Delta y'_C = 0. \tag{8}$$

That is to say, however big or small the misalignment angles brought by the three spherical mirrors and the three planar mirrors are, Eq. (8) will always be valid. We use the functions of $x'_A(t)$, $y'_A(t)$, $x'_B(t)$, $y'_B(t)$, and $x'_C(t)$, $y'_C(t)$ to represent the optical-axis locations at the time of t. When $t = 0$, the optical-axis locations at points P_A, P_B, and P_C can be written as $x'_A(0)$, $y'_A(0)$, $x'_B(0)$, $y'_B(0)$, and $x'_C(0)$, $y'_C(0)$. The optical-axis perturbations during the period of time from 0 to t can be written as

$$\Delta x'_A(0 \to t) = x'_A(t) - x'_A(0),$$
$$\Delta y'_A(0 \to t) = y'_A(t) - y'_A(0),$$
$$\Delta x'_B(0 \to t) = x'_B(t) - x'_B(0),$$
$$\Delta y'_B(0 \to t) = y'_B(t) - y'_B(0),$$
$$\Delta x'_C(0 \to t) = x'_C(t) - x'_C(0),$$
$$\Delta y'_C(0 \to t) = y'_C(t) - y'_C(0). \tag{9}$$

According to Eq. (8),

$$\Delta x'_A(0 \to t) + \Delta y'_A(0 \to t) + \Delta x'_B(0 \to t) + \Delta y'_B(0 \to t) + \Delta x'_C(0 \to t) + \Delta y'_C(0 \to t) = 0. \tag{10}$$

From Eq. (9), we can obtain

$$x'_A(t) + y'_A(t) + x'_B(t) + y'_B(t) + x'_C(t) + y'_C(t) = x'_A(0) + y'_A(0) + x'_B(0) + y'_B(0) + x'_C(0) + y'_C(0). \tag{11}$$

Equation (11) is always valid at any time of t for an ideal triaxial ring resonator. In fact, because there has always been the machining error in any actual resonator, Eq. (12) should be equal to a constant for a real triaxial ring resonator and we could define the constant as C:

$$x'_A(t) + y'_A(t) + x'_B(t) + y'_B(t) + x'_C(t) + y'_C(t) = C. \tag{12}$$

The value of the constant C is not changeable with the misalignment of any spherical mirror or planar mirror. The machining angle error of any terminal surface of a resonator can be equivalent to the misalignment angle of the terminal mirror. When a triaxial ring resonator has been machined, its value of C cannot be decreased by modifying the angles of the terminal surfaces or the terminal mirrors. We can call this constant C the mismatchining error of the triaxial ring resonator. The smaller the value of C, the smaller the mismatching error. When $C = 0$, the mismatching error is 0 and it is an ideal triaxial ring resonator.

Because the mismatching error C of an actual triaxial ring resonator is always not equal to 0, we need to find out an optimization method to share the mismatching error. By utilizing Eqs. (6)–(8), the distances between the optical axis and the center of the diaphragm at any point of P_A, P_B, and P_C can be written as D_A, D_B, and D_C,

$$D_A = \sqrt{x_A^2 + y_A^2} = \sqrt{x_A'^2 + 4y_A'^2},$$
$$D_B = \sqrt{x_B^2 + y_B^2} = \sqrt{x_B'^2 + 4y_B'^2},$$
$$D_C = \sqrt{x_C^2 + y_C^2} = \sqrt{x_C'^2 + 4y_C'^2}. \tag{13}$$

Obviously, the three monoaxial ring resonators cannot be aligned to the best condition of $D_A = D_B = D_C = 0$ simultaneously because $C \neq 0$. To make the total diffraction loss of the monolithic triaxial ring resonator the lowest, the values of D_A, D_B, and D_C should be simultaneously made the smallest. That is to say that the mismatching error should be shared equally. So the best case should be

$$x'_A(t) = x'_B(t) = x'_C(t) = C/3,$$
$$y'_A(t) = y'_B(t) = y'_C(t) = 0,$$
$$D_A = D_B = D_C = \frac{|C|}{3}. \tag{14}$$

If we let the mismatching error be shared equally by $y'_A(t)$, $y'_B(t)$, and $y'_C(t)$, then

$$y'_A(t) = y'_B(t) = y'_C(t) = C/3,$$
$$x'_A(t) = x'_B(t) = x'_C(t) = 0,$$
$$D_A = D_B = D_C = \frac{2}{3}|C|. \tag{15}$$

The following is another example of sharing the mismatching error:

$$x'_A(t) = -C/3, \qquad x'_B(t) = C, \qquad x'_C(t) = C/3,$$
$$y'_A(t) = y'_B(t) = y'_C(t) = 0,$$
$$D_A = \frac{1}{3}|C|, \qquad D_B = |C|, \qquad D_C = \frac{1}{3}|C|. \tag{16}$$

Obviously the first case is better than the next two cases.

3. Conclusions

In conclusion, a criterion C, which represents the mismatching error of the monolithic triaxial ring resonator, has been found. It is basic that the machining accuracy should be enhanced to decrease the mismatching error C. The mismatching error C of the triaxial ring resonator cannot be decreased by modifying the angles of the terminal surfaces or the terminal mirrors. When $C \neq 0$, the three monoaxial ring resonators cannot be aligned to the best condition simultaneously. An optimization method to share the mismatching error C has been proposed. The method is to share the mismatching error C in the three specific directions of x_A, x_B, and x_C equally and simultaneously. By utilizing this method, the alignment precision can be greatly improved and the total diffraction loss will be lowest in any monolithic triaxial ring resonator.

The authors gratefully acknowledge the support from the National Science Foundation of China under grant 60608002.

References

1. W. W. Chow, J. Gea-Banacloche, L. M. Pedrotti, V. E. Sanders, W. Schleich, and M. O. Scully, "The ring laser gyro," Rev. Mod. Phys. **57,** 61–86 (1985).
2. M. Faucheux, D. Fayoux, and J. J. Roland, "The ring laser gyro," J. Opt. (Paris) **19,** 101–115 (1988).
3. A. E. Siegman, "Laser beams and resonators: beyond the 1960s," IEEE J. Sel. Top. Quantum Electron. **6,** 1389–1399 (2000).
4. M. L. Stitch and M. Bass, *Laser Handbook* (North-Holland, 1985), Vol. 4, Chap. 3, pp. 229–332.
5. A. H. Paxton and W. P. Latham, "Unstable resonators with 90° beam rotation," Appl. Opt. **25,** 2939–2946 (1986).
6. J. A. Arnaud, "Degenerate optical cavities. II. Effects of misalignments," Appl. Opt. **8,** 1909–1917 (1969).
7. G. B. Altshuler, E. D. Isyanova, V. B. Karasev, A. L. Levit, V. M. Ovchinnikov, and S. F. Sharlai, "Analysis of misalignment sensitivity of ring laser resonators," Sov. J. Quantum Electron. **7,** 857–859 (1977).
8. I. W. Smith, "Optical resonator axis stability and instability from first principles," in *Fiber Optic and Laser Sensors,* Proc. SPIE **412,** 203–206 (1983).
9. A. L. Levit and V. M. Ovchinnikov, "Stability of a ring resonator with a nonplane axial contour," J. Appl. Spectrosc. **40,** 657–660 (1984).
10. S.-C. Sheng, "Optical-axis perturbation singularity in an out-of-palne ring resonator," Opt. Lett. **19,** 683–685 (1994).
11. J. Yuan, X. Long, B. Zhang, F. Wang, and H. Zhao, "Optical axis perturbation in folded planar ring resonators," Appl. Opt. **46,** 6314–6322 (2007).
12. A. H. Paxton and W. P. Latham, Jr., "Ray matrix method for the analysis of optical resonators with image rotation," Proc. Soc. Photo-Opt. Instrum. Eng. **554,** 159–163 (1985).
13. R. Rodloff, "A laser gyro with optimized resonator geometry," IEEE J. Quantum Electron. **QE-23,** 438–445 (1987).
14. J. Yuan and X. W. Long, "Optical-axis perturbation in nonplanar ring resonators," Opt. Commun. **281,** 1204–1210 (2008).
15. J. C. Stiles and B. H. G. Ljung, "Monolithic three axis ring laser gyroscope," U.S. patent 4,477,188 (16 October 1984).
16. A. E. Siegman, *Lasers* (University Science, 1986), Chap. 15.
17. A. Gerrard and J. M. Burch, *Introduction of Matrix Methods in Optics* (Gersham, 1975).